Regulation of the Fast Vacuolar Channel by Cytosolic and Vacuolar Potassium

Igor I. Pottosin* and Manuel Martínez-Estévez†
*Centro Universitario de Investigaciones Biomédicas, Universidad de Colima, 28047 Colima, Col., México; and †Centro de Investigación Científica de Yucatán, 97200 Mérida, Yucatán, Mexico

ABSTRACT At resting cytosolic Ca^{2+}, passive K^+ conductance of a higher plant tonoplast is likely dominated by fast vacuolar (FV) channels. This patch-clamp study describes K^+-sensing behavior of FV channels in *Beta vulgaris* taproot vacuoles. Variation of K^+ between 10 and 400 mM had little effect on the FV channel conductance, but a pronounced one on the open probability. Shift of the voltage dependence by cytosolic K^+ could be explained by screening of the negative surface charge with a density $\sigma = 0.25\ e^-/nm^2$. Vacuolar K^+ had a specific effect on the FV channel gating at negative potentials without significant effect on closed-open transitions at positive ones. Due to K^+ effects at either membrane side, the potential at which the FV channel has minimal activity was always situated at ~50 mV below the potassium equilibrium potential, E_{K^+}. At tonoplast potentials below or equal to E_{K^+}, the FV channel open probability was almost independent on the cytosolic K^+ but varied in a proportion to the vacuolar K^+. Therefore, the release of K^+ from the vacuole via FV channels could be controlled by the vacuolar K^+ in a feedback manner; the more K^+ is lost the lower will be the transport rate.

INTRODUCTION

K^+ is the most abundant cation species in cells of nonhalophyte plants. K^+ stored in the large central vacuole is a major cationic component of the cellular osmoticum, hence directly contributing to volume/turgor regulation underlying plant growth and responses to osmotic stress, as well as a variety of specialized functions, e.g., stomatal movements. In the vacuolar membrane, three cation-selective channels have been characterized to date. Two of them, the K^+-selective and the Ca^{2+}-permeable ones require elevated, few micromolar–100 micromolar levels of cytosolic Ca^{2+} for their activation (Ward and Schroeder, 1994; Allen and Sanders, 1996; Dobrovinskaya et al., 1999). Under resting cytosolic Ca^{2+} conditions, the channel of the third type, a so-called fast vacuolar (FV) one, represents the principal passive pathway for cations uptake and release across the vacuolar membrane (Allen and Sanders, 1996; Tikhonova et al., 1997; Allen et al., 1998; Brüggemann et al., 1999). Although the FV channel poorly selects between monovalent cations (Brüggemann et al., 1999), due to the abundance of K^+ it mainly operates as a K^+-conducting channel. FV channels are activated at extreme potentials of either sign, whereas around −40 mV they mainly reside in the closed state (Allen and Sanders, 1996; Tikhonova et al., 1997; Allen et al., 1998). However, this refers to the behavior in symmetrical K^+ conditions. Variation of the cytosolic K^+ appeared to shift the voltage dependence of FV currents both in *Vicia faba* guard cell and in barley mesophyll vacuoles (Allen and Sanders, 1996; Tikhonova et al., 1997). Vacuolar K^+ concentration displays much larger variability than the cytosolic one in vivo. Under conditions of severe K^+ deficiency, the cytosolic K^+ level in a variety of plant cells is kept fairly constant at the expense of the vacuolar K^+ pool (Leigh and Wyn Jones, 1984; Walker et al., 1996). Depending on the nutrient availability and metabolic status of the plant, K^+ may be substituted by other cations or by nonelectrolytes (Leigh, 1997). For instance, K^+ concentration in the open turgid stomata transiently drops ~threefold in the midday as compared to the maximal level achieved in the morning hours, whereas K^+ is replaced by sucrose to balance the decrease in osmotic pressure (Talbott and Zeiger, 1996). More profound decrease of vacuolar K^+ occurs in guard cells upon stomata closure, whereas neighboring epidermal cells experience an opposite change (Leigh, 1997). Does the variation of vacuolar K^+ affect the gating of the FV channel? What are the mechanisms of the FV channel regulation by vacuolar and cytosolic K^+? Finally, what might be the physiological impact of the K^+-sensing in this vacuolar K^+-conducting channel? To answer these questions we have studied the effects of the isoosmotic K^+ variation at either side of tonoplast on the FV channels.

MATERIALS AND METHODS

Preparation and media

Fresh *Beta vulgaris* (whole plants) were received from a local market and kept at +4°C before use. The osmolality of solutions was adjusted (range 680–730 mOs) to isotonic or slightly hypertonic with respect to the vacuolar sap by sorbitol as verified by a cryoscopic osmometer (OSMOMAT 030, Gonotec, Germany). Vacuoles have been isolated mechanically by cutting the taproot slices. Few released vacuoles were collected by a micropipette (5–10 μl volume) and transferred to the experimental chamber (300 μl volume). Experiments were carried out at room temperature (23–25°C); bath and pipette solutions contained 2 mM EGTA (free Ca^{2+} <2 nM) to abolish Ca^{2+}-activating ion channels and ensure exclusive registration of the FV current; pH was adjusted to 7.5 with HEPES (5–15 mM). Solutions with 10,

Submitted April 23, 2002, and accepted for publication October 21, 2002.
Address reprint requests to Dr. Igor Pottosin, Centro Universitario de Investigaciones Biomédicas, Universidad de Colima, Av. 25 de julio s/n, Villa de San Sebastián, 28047 Colima, Col., México. Tel.: +52-312-31-61000, x47456; Fax: +52-312-31-27581; E-mail: pottosin@cgic.ucol.mx.

0006-3495/03/02/977/10 $2.00

30, 100, and 400 mM K^+ were prepared by addition of the correspondent amount of KCl, taking into the account K^+ introduced by KOH titration of EGTA and HEPES. *N*-methyl-D-glucamine ($NMDG^+$) was titrated by HCl to neutral pH before use. All chemicals were analytical grade (Sigma, St Louis, MO).

Patch-clamp protocols and analyses

Patch pipettes were pulled from KIMAX-51 capillaries (Kimble, Toledo, Ohio) in three steps on a Brown/Flaming model P-97 puller (Sutter Instruments, Novato, CA), fire polished (LPZ 101 microforge, List Medical, Germany), and covered by Sylgard-curing agent (Dow Corning, Midland, MI). The resistance of patch electrodes filled with a 100-mM KCl solution was 2–3 MΩ; pipettes with higher resistance of 7–10 MΩ have been selected for single-channel recordings. Current measurements were performed using an Axopatch 200A integrating patch-clamp amplifier (Axon Instruments, Foster City, CA). Reference AgCl electrode was connected to the bath via 3% agar bridge filled with 100 mM KCl. The sign of voltage referred to the cytosolic side, and positive (outward) currents represented an efflux of cations into the vacuole. Liquid junction potential between reference electrode and solution containing 10 mM K^+ plus 90 mM $NMDG^+$, measured as described by Ward and Schroeder (1994), was $+7.1 \pm 0.1$ mV (bath positive). Large ($C = 0.5$–2 pF) outside-out and inside-out tonoplast patches, respectively, have been examined to test the effects of cytosolic and vacuolar K^+ on the FV current; K^+ concentration was changed by bath perfusion. The identity of the FV current was verified by its characteristic rapid (<1 ms) activation and bipolar voltage dependence, i.e., activation at large potentials of either sign, with a minimal open probability at around −40 mV in symmetrical K^+ (Tikhonova et al., 1997; Dobrovinskaya et al., 1999). The conductance in the high resistance region between −20 and −60 mV was taken as a measure of the membrane integrity and seal stability. Patches with the conductance >250 pS in this voltage region in symmetrical 100 mM KCl have been rejected from further analysis. From holding potential of −40 mV, voltage has been switched to a sequence of test potentials in 20-mV steps. Depending on the patch stability, the range of command potentials was from (−160, +140) mV up to ±200 mV. The amplitude of the FV current was measured at the first 5–10 ms of the test pulse after cessation of a small capacitance artifact. Each experiment has been started in symmetrical 100 mM K^+. To ensure the reversibility, at the end of the experiment symmetrical 100-mM K^+ conditions have been restored. The variation of FV current amplitudes between the beginning and the end of experiments was less than 20%.

Records were filtered at 5 kHz by a low-pass Bessel filter, digitized using a DigiData 1200 Interface (Axon Instruments), and recorded directly on a hard disk of an IBM-compatible PC at 15-kHz sampling rate. The command voltage protocols were applied and the analyses were carried out using the pClamp 6.0 software package (Axon Instruments). Voltage dependence of the FV channel was fitted to a three-state model with two open states connected via closed state as described by Tikhonova et al. (1997) with a modification:

$$\frac{P}{P(+100)} = \frac{A_1^* \exp(z_1^* F^* (V_1 - V)/RT) + A_2^* \exp(z_2^* F^* (V - V_2)/RT)}{1 + \exp(z_1^* F^* (V_1 - V)/RT) + \exp(z_2^* F^* (V - V_2)/RT)}, \quad (1)$$

where P and P(+100) are open probabilities at given potential/K^+ concentration and at +100 mV in symmetrical 100 mM K^+, respectively; A_1, A_2—open probability at infinite large negative and positive potentials; $z_1(V_1)$ and $z_2(V_2)$ are gating charge (midpoint potential) for negative and positive branches of voltage dependence; V is voltage, F, R, T have their usual meanings. Shift of midpoint potentials V_1 and V_2 due to the screening of surface charge at increased cation concentrations (Fig. 7 *a*) was described by modified Eq.17 (Latorre et al., 1992):

$$V_i(C) = V_{i(C=\infty)} + \phi_i(C) = V_{i(C=\infty)} - (2RT/F)^* \ln(X + (X^2 + 1)^{1/2}), \quad (2)$$

where $V_{i\ (C\ =\ \infty)}$ is "true" midpoint potential (in mV) at infinite cation concentration; $\phi_i(C)$ (in mV) is potential at zero distance from the surface as a function of concentration; and $X = 1.36^*\sigma^*C^{-1/2}$, σ is surface charge (in e^-/nm^2), and C is concentration (moles/liter).

RESULTS

To ensure the selective registration of the FV current, free concentration of divalent cations at both sides of vacuolar membrane were set to zero by the introduction of 2 mM EGTA into the nominally Ca^{2+} (and Mg^{2+}) free bath and patch pipette solutions. In the virtual absence of reducing agents and Mg^{2+}, low (<2 nM) cytosolic Ca^{2+} abolished the activity of Ca^{2+}-permeable and K^+-selective channels and favored that of FV (Allen and Sanders, 1996; Tikhonova et al., 1997; Carpaneto et al., 2001). At these conditions the rapidly activating FV current displays characteristic bipolar voltage dependence, i.e., increase of the macroscopic conductance at both positive and negative voltage steps from −40 mV, where the FV channel activity in symmetrical 100 mM KCl is minimal (Tikhonova et al., 1997; Allen et al., 1998; Dobrovinskaya et al., 1999). High patch resistance at voltages around −40 mV (Fig. 1) ruled out the substantial contribution of the unspecific leak, which is an important prerequisite for the correct evaluation of an instantaneously activating current.

Effects of the variation of cytosolic and vacuolar potassium concentration on FV currents are illustrated in Fig. 1. Macroscopic FV currents have been recorded on large outside (cytosolic side)-out and inside (vacuolar side)-out tonoplast patches (Fig. 1, *a* and *b*). Patch pipette solution in both cases contained 100 mM K^+. Corresponding current-voltage relations are presented on plots below each original experimental series. It can be seen from the records and current-voltage relations that the decrease of cytosolic K^+ from 400 mM to 10 mM caused a gradual positive shift of the FV current voltage dependence, i.e., the outward current became activated at more positive potentials and inward current at less negative ones (Fig. 1 *a*). At the same time, the decrease of the vacuolar K^+ caused an asymmetric effect: the suppression of the inward current without marked effect on the outward one (Fig. 1 *b*).

The change of the macroscopic current (I) may be produced either by a change of single-channel current amplitude (i), or by a variation of the mean number of open channels (NP_o, where N is number of channels and P_o is open probability), or by a combination of both factors, following the relation $I = i \times NP_o$. To clarify this issue, we have tested the effect of the variation of cytosolic (Fig. 2) and vacuolar (Fig. 3) K^+ on smaller patches with limited number of FV channel copies, where single-channel openings can be resolved. As it can be seen from Fig. 2, the decrease of

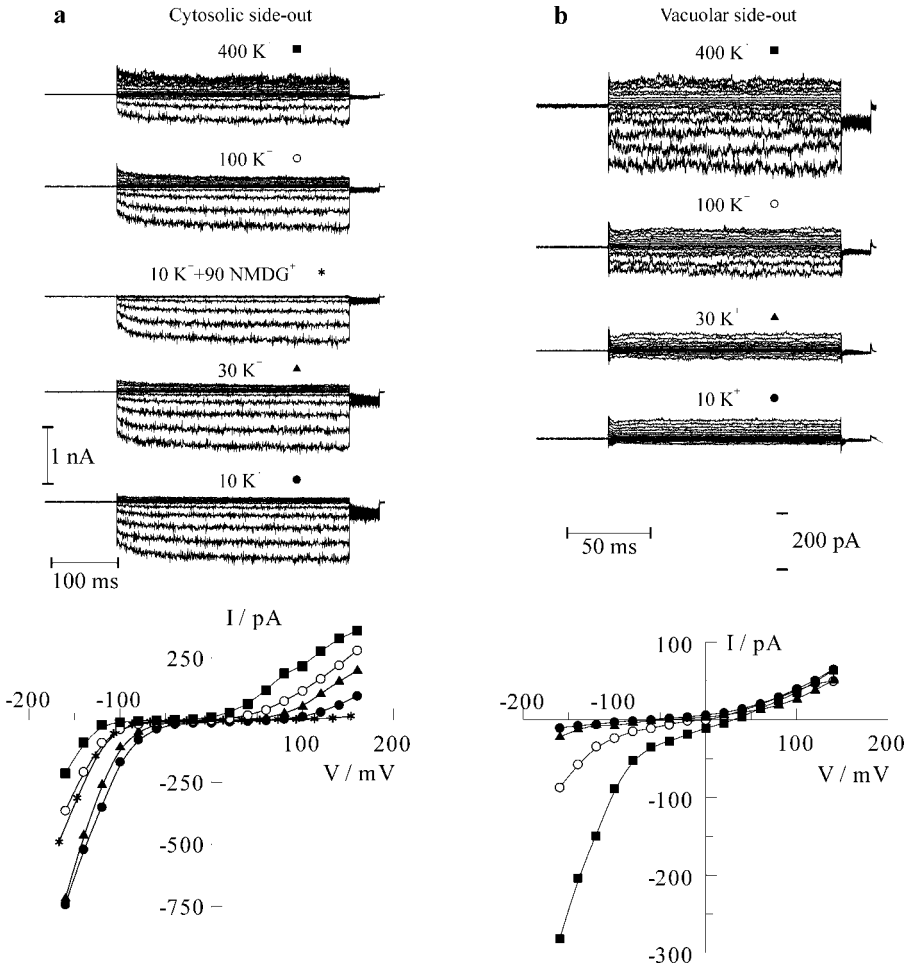

FIGURE 1 Macroscopic fast vacuolar (FV) currents in vacuoles of *Beta vulgaris* at different cytosolic and vacuolar K^+ concentrations. Original recordings and correspondent current-voltage relations on large cytosolic (*a*, $C \sim 1$ pF) and vacuolar (*b*, $C \sim 0.5$ pF) side-out patches. From holding value of -40 mV, the voltage was stepped to $\pm$ 160 mV with 20-mV increment; at the end of each step the voltage was switched to -100 mV. Pipette solution contained 100 mM K^+; cytosolic (*a*) and vacuolar (*b*) K^+ concentration (in mM) was varied by bath perfusion as indicated. In the case of solution containing 90 mM $NMDG^+$, voltage was corrected for the liquid junction potential between bath and reference electrode.

cytosolic K^+ from 100 to 10 mM caused a decrease of the mean number of open channels at positive potentials (+100 mV) and an increase of the probability of opening at negative ones (-75 mV). The latter effect of K^+ was unspecific, because the introduction of 90 mM of $NMDG^+$ on the background of 10 mM K^+ reversed the channel open probability at negative potentials to the level observed in symmetrical 100 mM K^+. However, $NMDG^+$ strongly inhibited the channel activity at positive potentials. Both effects of $NMDG^+$ on the single-channel activity are fairly comparable with those on the macroscopic FV currents (Fig. 1 *a*). The effects of cation variation at the cytosolic side on the channel gating have been reproduced on three additional small cytosolic side-out patches. Taking mean number of open channels in control (symmetrical 100 mM K^+) as a reference, the decrease of cytosolic K^+ to 10 mM caused the decrease of open probability at +100 mV by almost two-thirds (0.36 ± 0.05, $n = 4$), whereas the open probability at -75 mV was increased 3.71 times (± 0.18, $n = 4$). At the same time, the application of 10 mM K^+ supplemented by 90 mM $NMDG^+$ at the cytosolic side restored the open probability at -75 mV to the value of 0.97 ± 0.15 ($n = 4$) of that in control, whereas open probability at positive potentials was strongly (to the level <0.05 of that in control) reduced. Inspecting tiny vacuolar side-out patches then, it was found that the decrease of vacuolar K^+ from 100 to 10 mM hardly affected single channel activity at positive potentials (Fig. 3, +50), whereas at negative potentials (-150) the probability of the FV channel opening has been strongly reduced. Averaging data obtained on three separate vacuolar side-out patches yielded the open probability values (taken relative to control ones) of 1.17 ± 0.07 and 0.14 ± 0.02 at +50 mV and -150 mV, respectively. The decrease of the open probability at negative potentials and low K^+ could be reversed only partly by the addition of 90 mM $NMDG^+$ (0.43 ± 0.10 of the mean open channel number in control at -150 mV, $n = 2$) to the vacuolar side, which argued for some specificity of the monovalent cation (K^+ or $NMDG^+$) interaction with the channel gate.

The analysis, performed above, implied that both changes of the cytosolic and of the vacuolar K^+ caused substantial effects on the FV channel open probability. However, due to the fast flickering kinetics and relatively low unitary conductance, it was generally difficult to unravel precisely the mean number of open FV channels as a function of membrane voltage from amplitude histograms, especially at

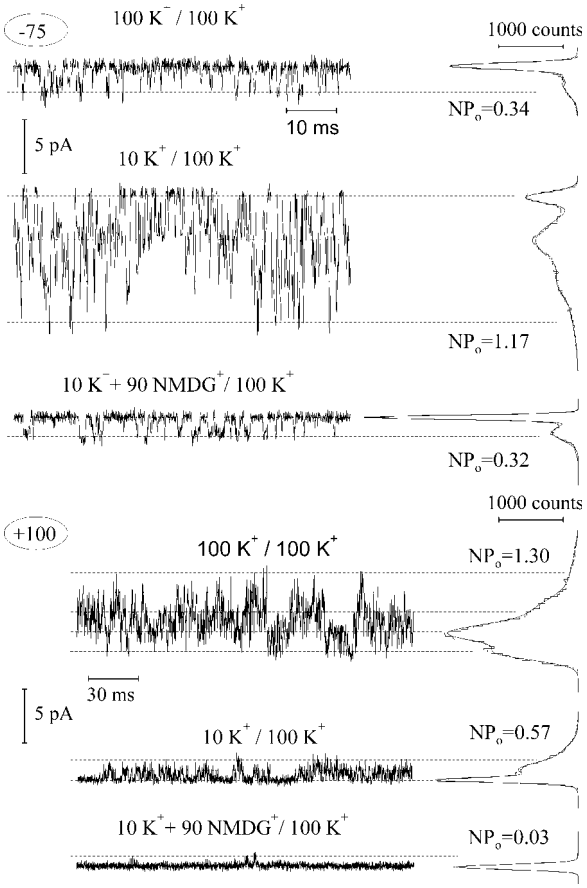

FIGURE 2 Effect of cytosolic K^+ on the activity of single FV channels. Records (5 kHz filtering, 15.2 kHz sampling) were performed on a tiny cytosolic side-out patch, containing ≥4 copies of active FV channels. Cytosolic/vacuolar cation concentrations (in mM) are indicated above and membrane voltage at the left of each original record. Data at positive (+100 mV) voltage were additionally low-pass filtered at 2.5 kHz and presented in a three-times condensed timescale to show long-lasting channel closures. Amplitude histograms at the right side of each record were constructed over ~2-s long record and fitted by a sum of Gauss functions to obtain mean number of open channels (NP_o). Dashed lines indicate mean current levels for zero (leak) up to four channels open.

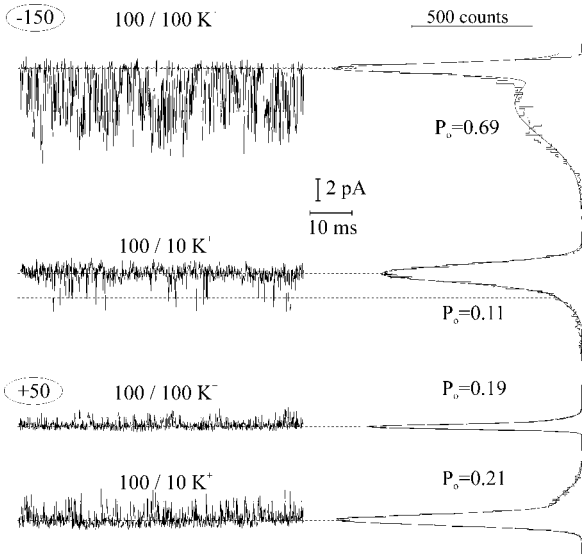

FIGURE 3 Effect of vacuolar K^+ on the activity of single FV channel. Records (5 kHz filtering, 15.2 kHz sampling) were performed on a tiny vacuolar side-out patch. Cytosolic/vacuolar cation concentrations (in mM) are indicated above and membrane voltage at the left of each original record. Amplitude histograms at the right side of each record were constructed over ~1-s long record and fitted by a sum of two Gaussians to obtain the mean open probability (P_o). Dashed lines indicate the mean current level with no or one channel open.

high or very low channel activity. Alternatively, short stretches of single FV channel recordings were manually evaluated to construct unitary current-voltage relations at different K^+ gradients. Example of single-channel recording on a small outside-out patch bathed in 10 mM K^+ and 100 mM solutions at the cytosolic and vacuolar side, respectively, is presented in Fig. 4 *a*. Single-channel currents as a function of membrane voltage for 400, 100, 30, and 10 mM cytosolic K^+ and also for 10 mM K^+ plus 90 mM $NMDG^+$ against 100 mM vacuolar K^+ are plotted in Fig. 4 *b*. Same solution series, now at the vacuolar side against fixed 100 mM K^+ at the cytosolic side, have been tested also on small inside-out patches containing few FV channel copies (Fig. 4 *c*). Variation of K^+ concentration in the range from 10 to 400 mM did not cause large changes in the slope of current-voltage relations (Fig. 4, *b* and *c*). We have evaluated single-channel currents 100 mV more positive to the reversal potential in the case of cytosolic side-out patches or 100 mV more negative in the case of vacuolar side-out patches to ensure that the current is dominated by K^+ efflux from cytosolic or vacuolar sides, respectively. Resulting current amplitudes are plotted as a function of cytosolic or vacuolar K^+ concentration (Fig. 4 *d*). Fitting data points to the Michaelis-Menten equation resulted in similar values of dissociation constants for cytosolic and vacuolar K^+, 5.6 ± 2.2 mM and 5.1 ± 1.9 mM. In other words, in the range of tested K^+ concentrations, the FV channel conductance almost reached the saturation level.

To quantify the effect of K^+ on the voltage-dependent open probability of the FV channel, we have divided macroscopic current-voltage relations as those presented in Fig. 1 by corresponding single-channel ones presented in Fig. 4, *b* and *c*. This procedure results in a mean number of open FV channels ($N \times P_o$) as a function of membrane voltage. Results (in relative units) for different levels of cytosolic and vacuolar K^+ are summarized in Fig. 5 and Fig. 6, respectively. Fig. 5 shows that the variation of the cytosolic K^+ caused almost a parallel shift of the voltage dependence along the voltage axis, without marked changes of saturation levels reached at large positive and negative potentials, and of the minimal activity level. However, both saturation level at positive potentials and the minimal open probability were decreased upon application of 90 mM

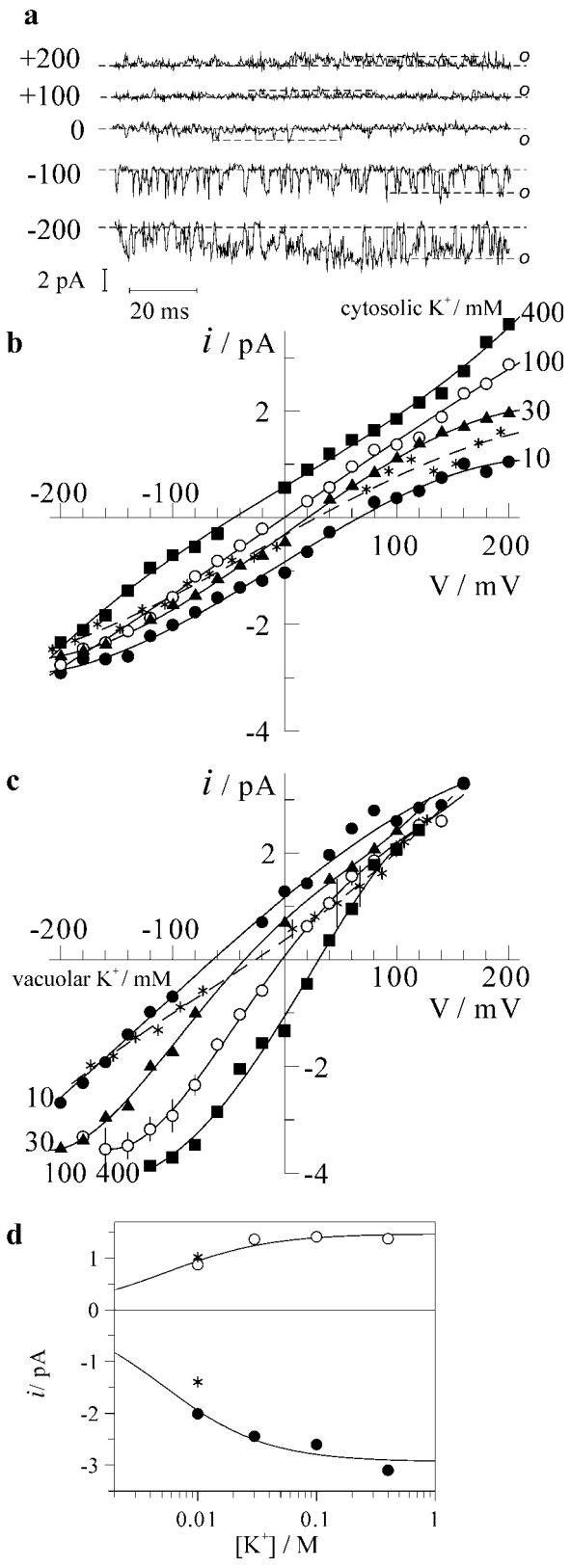

FIGURE 4 Effect of cytosolic and vacuolar K^+ on single-channel current-voltage relations. (*a*) Example of single-channel recording on a tiny cytosolic side-out patch bathed in 10-mM K^+ solution; patch pipette was filled with 100-mM K^+ solution. Traces were filtered at 1 kHz. Open channel level is indicated by *o*, dashed line is the baseline corresponding to the closed channel level. (*b*) Single-channel current amplitudes as a function of membrane voltage were measured in experiments as one presented (*a*). Pipette (*vacuolar side*) was filled with 100-mM K^+ solution; cytosolic side was bathed in solutions with variable K^+ as indicated (in mM); asterisks are data obtained in 10-mM K^+ plus 90-mM $NMDG^+$ solution. (*c*) Single-channel current-voltage relationships for vacuolar side-out patches. Pipette (*cytosolic side*) was filled with 100-mM K^+ solution, vacuolar K^+ concentrations (in mM) are indicated. For symmetric 100 mM K^+, $n = 5$ patches were analyzed and data are presented as mean ± SD. Those include also controls for two separate experiments where 10 mM K^+ supplemented by 90-$NMDG^+$ solution was tested (*asterisks*). (*d*) Single-channel current at potential 100 mV above (cytosolic side-out patch, *hollow symbols*) or below (vacuolar side-out patches, *filled symbols*) the reversal potential for single FV channel current as a function of cytosolic or vacuolar K^+. Data were fitted to Michaelis-Menten equation with dissociation constant values given in the text. Points for 10 mM K^+ supplemented by 90-mM $NMDG^+$ solution (*asterisks*) are given for the comparison.

$NMDG^+$ (Fig. 5 *b*), implying a destabilization of the open state occupied at cytosol positive potentials by this agent. Effect of vacuolar K^+ on the voltage dependence of the FV channel open probability displayed a different pattern (Fig. 6). The effect may be roughly described by preferential stabilization of the open state occupied at negative potentials. With the increase of vacuolar K^+, the transition between this open state and the closed one occurred at progressively positive potentials. When the shift approached the region of the channel activation by positive potentials (transition from the closed to the second open state), marked increment of the minimal open probability was observed (Fig. 6 *a*). To explain our results, curves have been adjusted to a pseudo three-state model with two distinct open states occupied at extreme potentials of either sign connected by voltage-dependent transitions via the closed state (Eq. 1 in Materials and Methods). Voltage-dependent transitions between the closed and each of the open states have been described by Boltzmann functions, yielding gating charge (z_1 or z_2) and midpoint potentials (V_1 or V_2) for the activation at negative or positive potentials, respectively. This analysis showed that the slope of the voltage dependence does not change in a systematic manner upon the variation of K^+, with values for z_1 and z_2 being in the range of 0.9–1.25 and 0.3–0.5, respectively. However, values of V_1 and V_2 or V_1 alone have been strongly affected by the variation of cytosolic or vacuolar K^+, respectively (Fig. 7). Analysis of this K^+ dependence allowed us to suggest differential mechanisms of the modulation of the FV channel voltage gating by cytosolic and vacuolar potassium.

DISCUSSION

Mechanisms of the fast vacuolar channel regulation by K^+

The effect of cytosolic K^+ on the FV channel gating can be described in simple terms: a parallel decrease with a slope of

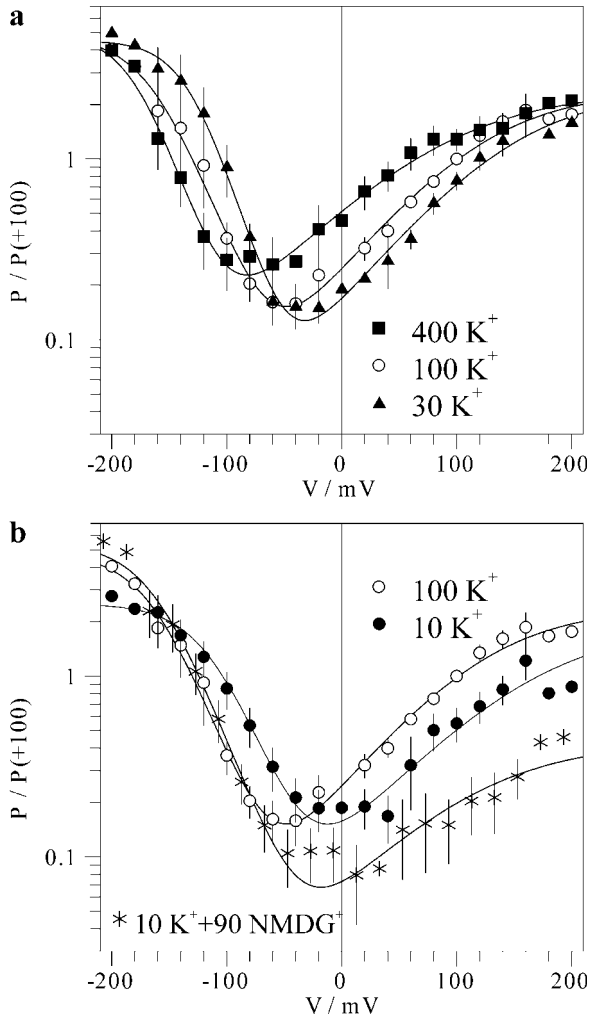

FIGURE 5 Effect of the cytosolic K^+ on the voltage dependence of the FV channel. Macroscopic FV current-voltage relations for 100-mM vacuolar K^+ and variable cytosolic K^+ as ones presented in Fig. 1 *a* were divided by corresponding single-channel current-voltage relations (Fig. 4) resulting in the mean number of open FV channels as the function of the voltage. Mean number of channels open at +100 mV in symmetric 100 mM K^+ was taken as a standard equal to 1 for each individual cytosolic side-out patch, and other data were scaled accordingly. The data for each cytosolic K^+ concentration obtained on *n* separate patches are averaged and presented as mean ± SD as a function of voltage. Symbols for 10 mM (*filled circles*, $n = 7$), 30 mM (*triangles*, $n = 5$), 100 mM (*hollow circles*, $n = 8$), and 400 mM (*squares*, $n = 5$) cytosolic K^+; 10 mM K^+ plus 90 mM $NMDG^+$ (*asterisks*, $n = 6$). Solid lines are best fits to the Eq. 1 given in Materials and Methods, with values of parameters V_1 and V_2 plotted in Fig. 7 *a*.

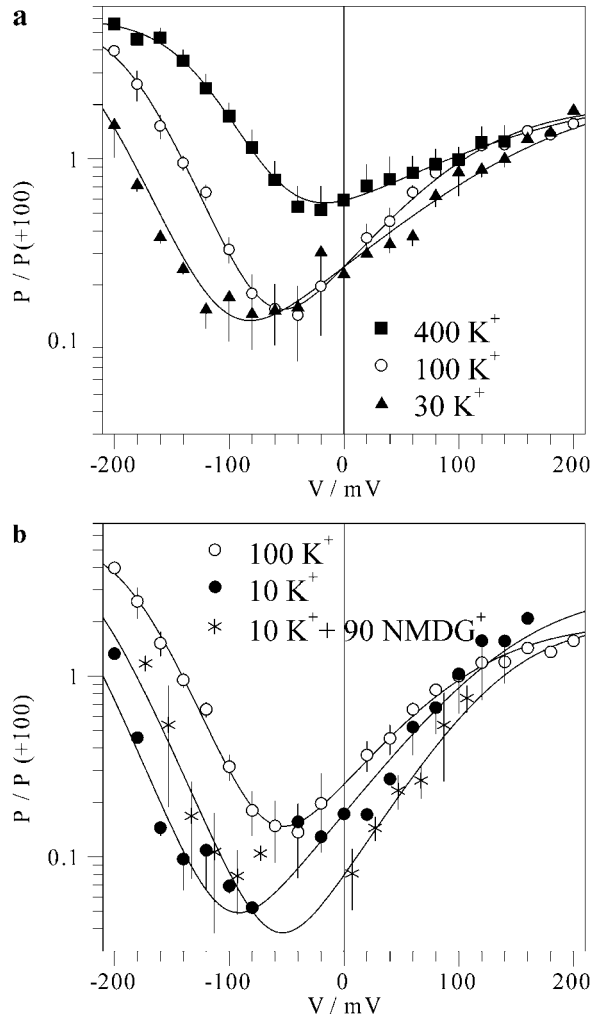

FIGURE 6 Effect of the vacuolar K^+ on the voltage dependence of the FV channel. Mean number of open FV channels (in relative units) at different vacuolar K^+ concentrations and 100 mM K^+ in the pipette (*cytosolic side*) as a function of membrane voltage were obtained as described in the Fig. 5 legend. The data for each vacuolar K^+ concentration obtained on *n* separate patches are averaged and presented as mean ± SD as a function of voltage. Symbols for different vacuolar K^+ concentrations: 10 mM (*filled circles*, $n = 3$), 30 mM (*triangles*, $n = 3$), 100 mM (*hollow circles*, $n = 6$), and 400 mM (*squares*, $n = 4$); 10 mM K^+ plus 90 mM $NMDG^+$ (*asterisks*, $n = 2$). Solid lines are best fits to Eq. 1, with values of parameters V_1 and V_2 plotted in Fig. 7 *b*.

~46 mV per a 10-fold increment of $[K^+]$ of both V_1 and V_2 (Fig. 7 *a*). The effect of the cytosolic K^+ increase from 10 to 100 mM on the V_1 and V_2 values could be mimicked by an equivalent increase of the ionic strength due to the addition of 90 mM $NMDG^+$ (*asterisk*, Fig. 7 *a*). These observations argue for a substantial negative surface potential at the cytosolic face of the channel. Fitting the dependence of V_1 and V_2 on cytosolic $[K^+]$ to a simple Gouy-Chapman model (Eq. 17, Latorre et al., 1992) yielded the surface charge density $\sigma \sim 0.25$ e^-/nm^2 (Fig. 7 *a*), which at 100 mM cytosolic $[K^+]$ will generate a surface potential of ~−45 mV. The estimated negative charge density is somewhat higher than that at the internal surface of voltage-dependent channels in animal cells and is in the range of the values reported for the external surface (Hille, 1992). It should be noted here that the surface potential is a local phenomenon, and much of the charge resides in the channel protein rather than at the surface of a phospholipid membrane. Indeed, the average density of the negative charge associated with the tonoplast of red beet, as calculated basing on the electro-

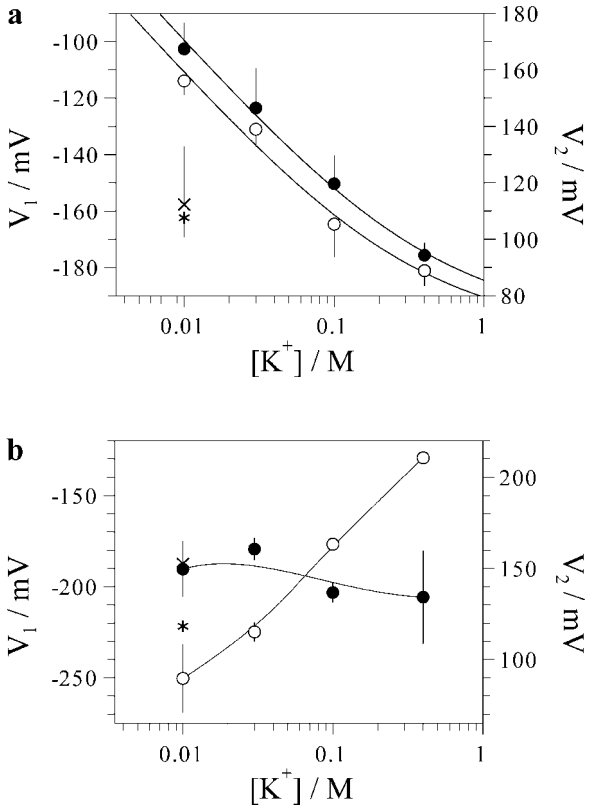

FIGURE 7 Effect of cytosolic and vacuolar K^+ on midpoint potentials of the voltage dependence of the FV channel. Values of midpoint potentials V_1 and V_2 for the gating processes at negative (*hollow circles, left axis*) and positive (*filled circles, right axis*) voltages, respectively, were obtained by fitting of the data presented in Figs. 5 and 6 to Eq. 1. Summary of results for the cytosolic (*a*) and for the vacuolar (*b*) K^+ variations are presented. Data in (*a*) were fitted to Eq. 2 yielding values for surface charge density (in e^-/nm^2) of 0.23 ± 0.06 and 0.27 ± 0.05, and limits for parameters V_1 and V_2 of −206 ± 10 mV and 67 ± 7 mV at infinite ion concentration, respectively. Solid lines connecting points in (*b*) have no theoretical meaning. Values of parameter V_1 (*) and V_2 (*x*) for 10 mM K^+ plus 90-mM $NMDG^+$ solution are included for the comparison.

phoretic mobility of membrane vesicles (Gibrat et al., 1985), was five times lower than the value of the cytosolic surface charge apparently ''seen'' by the FV channel voltage gate. Despite its universal application, surface charge theory is mainly ignored by plant membrane biologists. However, the effect of surface charge on the uptake of Ni^{2+} by mung beet root protoplasts has been recently reported (Zhang et al., 2001).

The increase of vacuolar K^+ from 10 to 400 mM caused a drastic (>120 mV) positive shift of the midpoint potential V_1 for the equilibrium between open state occupied at negative potentials and the closed state (Fig. 7 *b*). At the same time, the second voltage-gating process, taking place at positive potentials, was hardly altered. The mean value of V_2 even slightly decreased. Such an asymmetric effect on the two voltage-dependent gating processes in the FV channel cannot be explained solely by screening of the surface charge, which could only cause an equivalent shift of all voltage-dependent processes in the same direction. The simplest explanation of the vacuolar K^+ effect is that K^+ binding to an allosteric site overstabilized the open state occupied at cytosol-negative potentials (this might be, for instance, due to the voltage-dependent binding to this site) with respect to the closed and other open states. Alternatively, the effect of vacuolar K^+ increase might be also the combination of the surface charge screening (shifting the voltage dependence more positive) and a voltage-independent stabilization of both open states with respect to the closed state, so that the two effects on the open probability will sum up or cancel each other at negative or positive potentials, respectively.

Although surface charge theory considerations so far provided the most economic explanation of the effect of cytosolic K^+ on the FV channel voltage dependence, and an allosteric K^+ binding seemed to be a cause of the vacuolar K^+ effect, alternative (or complementary) mechanisms, where binding of a K^+ ion inside the pore affects the distribution between conducting and nonconducting conformations, could not be ruled out. Such models are receiving increased support inasmuch as new facts on the control of K^+ channels' gating by permeable or blocking cations bound within the pore are unraveled. There is mounting evidence that K^+ bound within the selectivity filter in the voltage-dependent K^+ channels acts as an open structure stabilizer, preventing their collapse to the *C*-type inactivated and defunct states (Kiss and Korn, 1998; Melishchuk et al., 1998). Recent x-ray crystallographic study revealed marked changes of the ion coordination structure in the selectivity filter of the KcsA K^+ channel in low K^+ solutions, so that the filter operation may be coupled to the channel's gating via local changes of K^+ concentration (Zhou et al., 2001). K^+ modulation of the instantaneous activation of an outwardly rectifying TOK1 channel in the yeast plasma membrane is another example of a gating-permeation coupling. The voltage dependence of the TOK1 was a function of the ratio of internal to external K^+ irrespective to the absolute K^+ concentrations, cf. the dependence of the onset of the FV channel voltage activation on E_{K^+} (Fig. 8 *a*). It was speculated that K^+ binding to the external end of the selectivity filter locks the TOK1 channel in the closed state, and K^+ binding to the inner side is coupled to the channel opening, either via repelling the external K^+ ion or by inducing the permissive filter conformation, allowing K^+ conductance in either direction (Loukin and Saimi, 1999). The effect of K^+ can be fairly mimicked by its closest analogs, Rb^+ and Cs^+, but hardly by impermeable Na^+ or $NMDG^+$ (Bertl et al., 1998; Vergani et al., 1998; Loukin and Saimi, 1999). Interestingly, the variation of the cation species at the cytosolic side had a pronounced effect on the open probability of the weakly selective FV channel—the lesser was the relative permeability, the lower was the open probability. Substitution of

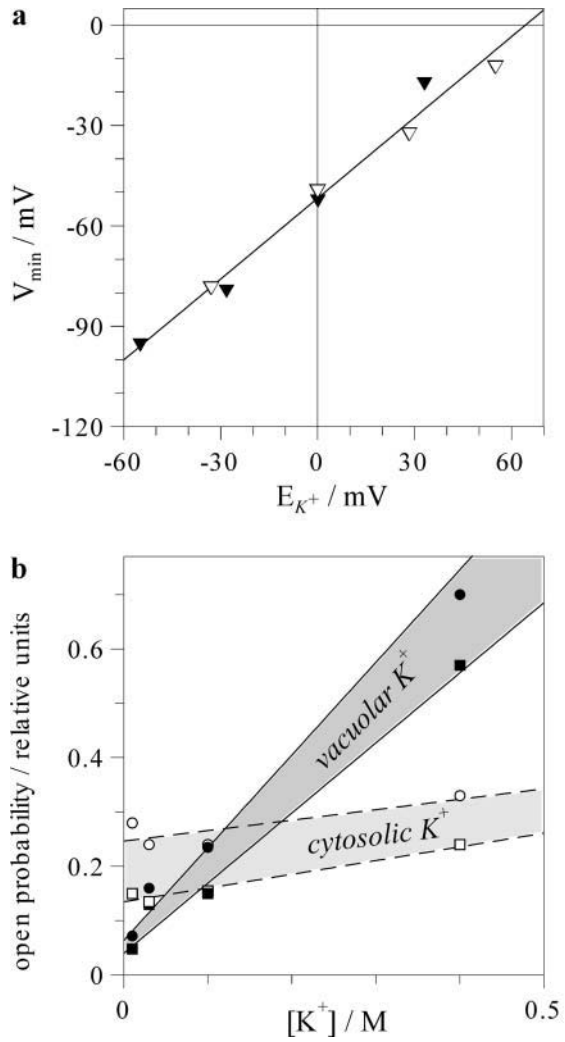

FIGURE 8 Relation between the minimum of voltage dependence and equilibrium potential for K^+ (*a*) and dependence on K^+ of the open probability of the FV channel in voltage range between these two points (*b*). (*a*) For each combination of the vacuolar and cytosolic K^+, the value of E_{K^+} was defined by Nernst equation. Voltage corresponding to the minimum of the voltage dependence was evaluated using plots in Figs. 5 and 6, and resulting values for cytosolic (*hollow symbols*) and vacuolar (*filled symbols*) K^+ variation were presented as a function of E_{K^+}. Solid line is linear regression with a slope 0.81 ± 0.05. (*b*) Open probability in the minimum of voltage dependence (*squares*) and at the potential equal to E_{K^+} (*circles*) were evaluated numerically using graphs in Figs. 5 and 6 and plotted as a function of cytosolic (*hollow symbols*) or vacuolar (*filled symbols*) K^+.

K^+ for less-permeable cations (Li^+ and Na^+) at the cytosolic side caused more destabilization of the open state occupied at negative membrane potentials than that occupied at positive ones (Brüggemann et al., 1999). In contrast to this, the substitution of K^+ by $NMDG^+$ at the cytosolic side selectively destabilized the open state occupied at positive potentials without any effect on closed-open transitions at negative potentials (Figs. 1 *a* and 2). None of these effects matched the effect of lowering the K^+ concentration. However, the effect of K^+–$NMDG^+$ substitution at the vacuolar side could be roughly mimicked by lowering of K^+ from 100 mM to 30 mM (Fig. 6 *b*); both these changes caused an equivalent shift of the reversal potential for the single-channel current (Fig. 4 *c*), i.e., the effect of $NMDG^+$ on the voltage dependence of the FV channel in this case was consistent with the relative permeability for this cation. Obviously, to account for the cation-specific interactions in the FV channel, the diverse effects of monovalent cations other than K^+ on gating and permeation need to be studied in depth.

Possible physiological implications of the FV channel control by K^+

Regulation of the FV channel by vacuolar and cytosolic K^+ provides a link between the equilibrium potential for K^+ (E_{K^+}) and the voltage dependence. Indeed, the minimum of voltage dependence was always situated by ~50 mV below E_{K^+} (Fig. 8 *a*). The effect of the cytosolic K^+ reported here is in a good agreement with previous reports on the tonoplast of *Vicia faba* guard cells and of barley mesophyll vacuoles (Allen and Sanders, 1996; Tikhonova et al., 1997). In addition, the present study shows that the relation between E_{K^+} and position of the minimum of the voltage dependence holds also for the case of the vacuolar K^+ variation. The shift of the voltage dependence, following that of E_{K^+}, is also a common feature of plasma membrane K^+ channels of different origin. Some channels as TOK1 respond to the variation of external and internal K^+ (Loukin and Saimi, 1999), whereas others to external K^+ only (Lopatin and Nichols, 1996; Blatt and Gradmann, 1997; Maathuis et al., 1997). Also specific mechanisms, underlying K^+-sensing, may be quite different: a destabilization of the polyamine binding within the pore of inward rectifier K^+ channels in animal cells (Lopatin and Nichols, 1996), gating-conductance coupling in yeast TOK1 channel (Loukin and Saimi, 1999), or an allosteric regulation of the plant outward rectifier by K^+ (Blatt and Gradmann, 1997). All in all, K^+ sensing by membrane transporters seems to be especially important for plants and fungi, which, in contrast with animals, need to maintain intracellular K^+ homeostasis under widely different ionic environments. Thus, K^+-sensing in the FV channel needs to be interpreted in the context of the physiological variation of K^+ gradient across the tonoplast.

In the physiological range of K^+ concentrations, the conductance of single FV channel in red beet vacuoles is almost constant (Fig. 4, *b–d*). Thus, the amplitude of the whole vacuole FV current depends mainly on the open probability of the channel and the offset of the membrane voltage from E_{K^+}, ($V_m - E_{K^+}$). In plant cells, potential difference across the tonoplast, reported by microelectrodes, ranged between 0 and −25 mV, which, in conjunction with K^+ gradients existing across the vacuolar membrane, implies moderate or negligible K^+-driving force directed from the

vacuole to the cytosol (Bethmann et al., 1995; Allen and Sanders, 1997). We hypothesized that the tonoplast potential is normally defined by a compromise between the activity of H^+-pumps, making it more negative and the shunt conductance through the K^+-permeable FV channel, shifting it toward E_{K^+} (cf. Davies and Sanders, 1995). Thus, the upper limit may be defined by E_{K^+}. And the lower limit would be situated close to the potential of the FV channel activity minimum. Indeed, further hyperpolarization will be reversed, because the pump-generated outward current, whose reversal is very negative (Gambale et al., 1994), will decrease, whereas the inward current through FV channels will steeply increase, causing a repolarization of the membrane voltage. Although the considerations made above delineate perhaps too broad (>50 mV width, Fig. 8 *a*) voltage range for possible values of tonoplast potentials, it can be shown that the open probability in this range undergoes only moderate variation. We have evaluated the FV open probability at E_{K^+} and at the minimum of the voltage dependence and plotted resulting values (Fig. 8 *b*) as a function of the vacuolar and cytosolic K^+. It can be immediately seen that within the selected potential range, the open probability of the FV channel weakly depends on voltage or cytosolic K^+, and strongly on the vacuolar K^+. Therefore, a simple conclusion may be drawn: a higher vacuolar K^+ implies a higher activity of the FV channels, and vice versa, the loss of vacuolar K^+ content induces the FV channel closure.

Feedback control of the vacuolar $^{86}Rb^+$ tracer release has been detected experimentally during ABA-induced stomatal closure (MacRobbie, 1995). The cessation of the release was achieved due to a solute content-sensitive behavior of vacuolar or plasma membrane ion channels. It was hypothesized then that some stretch-activated channels are involved (MacRobbie, 1998). Although our data do not rule out this possibility, they obviously provide another suitable explanation. The FV channel is highly permeable to Rb^+ (Brüggemann et al., 1999) and proposed to contribute significantly to the vacuolar solute loss in the course of ABA-induced stomatal closure (Allen et al., 1998). Therefore, the solute release may be regulated in a feedback manner via K^+-sensing mechanism of the FV channel. Interestingly, the activating voltage for plant plasma membrane K^+ channels is also changed in parallel with E_{K^+}, thus, they function as K^+-sensing valves. This property ensures that inwardly rectifying K^+ channels mediate K^+ uptake only, even at very low external K^+ (Maathuis et al., 1997). Similarly, activation threshold of outwardly rectifying K^+ channels in guard cells is always above E_{K^+}, which prevents K^+ reuptake at elevated external K^+, engaging solute loss and stomatal closure (Blatt and Gradmann, 1997).

In K^+-starved barley roots, K^+ in the cytosol was maintained at ~75 mM level, whereas the vacuolar K^+ activity dropped from 100 mM to <10 mM (Leigh and Wyn Jones, 1984; Walker et al., 1996). At the same time, membrane potential hardly changed, thus, electrochemical gradient for K^+ across the tonoplast was reversed (Walker et al., 1996). Obviously, the tonoplast passive conductance for K^+ needs to be minimized to prevent the reuptake of cytosolic K^+ into the vacuole. This may be partly achieved due to the downregulation of FV channels by reduced K^+ (Fig. 8 *b*). There are two additional factors contributing in the long-term scale to the maintenance of a low FV channel activity at K^+ starving conditions: the acidification of the cytosol (Walker et al., 1996) and drastic (up to 10 mM) increase of the putrescine level (Murty et al. 1971; Watson and Malmberg, 1996). Both factors were proved to inhibit the FV channel activity (Allen et al., 1998; Brüggemann et al., 1998; Dobrovinskaya et al., 1999).

We thank Dr. Gerald Schönknecht for the critical reading of the manuscript and extensive remarks, Dr. Oxana Dobrovinskaya for her participation in initial experiments, and Drs. Teresa Hernández and Jesús Muñiz for continuous support.

This work was funded by CONACyT grants 29473-N and 38181-N to I.I.P. and a fellowship from the grant 29473-N to M.M.

REFERENCES

Allen, G. J., and D. Sanders. 1996. Control of ionic currents in guard cell vacuoles by cytosolic and luminal calcium. *Plant J.* 10:1055–1069.

Allen, G. J., and D. Sanders. 1997. Vacuolar ion channels of higher plants. *Adv. Bot. Res.* 25:217–252.

Allen, G. J., A. Amtmann, and D. Sanders. 1998. Calcium-dependent and calcium independent K^+ mobilization channels in *Vicia faba* guard cell vacuoles. *J. Exp. Bot.* 49:305–318.

Bertl, A., H. Bihler, J. D. Reid, C. Kettner, and C. L. Slayman. 1998. Physiological characterization of the yeast plasma membrane outward rectifying K^+ channel DUK1 (TOK1), in situ. *J. Membr. Biol.* 162: 67–80.

Bethmann, B., M. Thaler, W. Simonis, and G. Schönknecht. 1995. Electrochemical potential gradients of H^+, K^+, Ca^{2+}, and Cl^- across the tonoplast of the green alga *Eremosphaera viridis*. *Plant Physiol.* 109:1317–1326.

Blatt, M. R., and D. Gradmann. 1997. K^+-sensitive gating of the K^+ outward rectifier in *Vicia* guard cells. *J. Membr. Biol.* 158:241–256.

Brüggemann, L. I., I. I. Pottosin, and G. Schönknecht. 1998. Cytoplasmic polyamines block the fast-activating vacuolar cation channel. *Plant J.* 16:101–106.

Brüggemann, L. I., I. I. Pottosin, and G. Schönknecht. 1999. Selectivity of the fast activating vacuolar cation channel. *J. Exp. Bot.* 50:873–876.

Carpaneto, A., A. M. Cantú, and F. Gambale. 2001. Effects of cytoplasmic Mg^{2+} on slowly activating channels in isolated vacuoles of *Beta vulgaris*. *Planta.* 213:457–468.

Davies, J., and D. Sanders. 1995. ATP, pH and Mg^{2+} modulate a cation current in *Beta vulgaris* vacuoles: a possible shunt conductance for the vacuolar H^+-ATPase. *J. Membr. Biol.* 145:75–86.

Dobrovinskaya, O. R., J. Muñiz, and I. I. Pottosin. 1999. Inhibition of vacuolar ion channels by polyamines. *J. Membr. Biol.* 167:127–140.

Gambale, F., H. A. Kolb, A. M. Cantú, and R. Hedrich. 1994. The voltage-dependent H^+-ATPase of the sugar beet vacuole is reversible. *Eur. Biophys. J.* 22:399–403.

Gibrat, R., H. Barbier-Brygoo, J. Guern, and C. Grignon. 1985. Transtonoplast potential difference and surface potential of isolated vacuoles. *In* Biochemistry and Function of Vacuolar Adenosine-Triphosphatase in Fungi and Plants. B.P. Marin, editor. Springer-Verlag, Berlin. 83–97.

Hille, B. 1992. Ionic Channels of Excitable Membranes, 2nd ed. Sinauer Associates, Sunderland, MA

Kiss, L., and S. J. Korn. 1998. Modulation of C-type inactivation by K^+ at the potassium channel selectivity filter. *Biophys. J.* 74:1840–1849.

Latorre, R., P. Labarca, and D. Naranjo. 1992. Surface charge effects on ion conduction in ion channels. *In* Methods in Enzymology, Vol. 207. Ion Channels. B. Rudy and L. E. Iverson, editors. Academic Press, San Diego. 471–501.

Leigh, R. A. 1997. Solute composition of vacuoles. *Adv. Bot. Res.* 25:171–194.

Leigh, R. A., and R. G. Wyn Jones. 1984. A hypothesis relating critical potassium concentrations for growth to the distribution and functions of this ion in the plant cell. *New Phytol.* 97:1–13.

Lopatin, A. N., and C. G. Nichols. 1996. [K^+] dependence of polyamine-induced rectification in inward rectifier potassium channels (IRK1, Kir 2.1). *J. Gen. Physiol.* 108:105–113.

Loukin, S. H., and Y. Saimi. 1999. K^+-dependent composite gating of the yeast K^+ channel, TOK1. *Biophys. J.* 77:3060–3070.

Maathuis, F. J. M., A. M. Ichida, D. Sanders, and J. I. Schroeder. 1997. Roles of higher plant K^+ channels. *Plant Physiol.* 114:1141–1149.

MacRobbie, E. A. C. 1995. Effects of ABA on $^{86}Rb^+$ fluxes at plasmalemma and tonoplast of stomatal guard cells. *Plant J.* 7:835–843.

MacRobbie, E. A. C. 1998. Signal transduction and ion channels in guard cells. *Phil. Trans. R. Soc. Lond. B.* 353:1475–1488.

Melishchuk, A., A. Loboda, and C. M. Armstrong. 1998. Loss of *Shaker* K channel conductance in 0 K^+ solutions: role of the voltage sensor. *Biophys. J.* 75:1828–1835.

Murty, K. S., T. A. Smith, and C. Bould. 1971. The relation between putrescine content and potassium status of black currant leaves. *Ann. Bot.* 35:687–695.

Talbott, L. D., and E. Zeiger. 1996. Central roles of potassium and sucrose in guard cell osmoregulation. *Plant Physiol.* 111:1051–1057.

Tikhonova, L. I., I. I. Pottosin, K. J. Dietz, and G. Schönknecht. 1997. Fast-activating cation channel in barley mesophyll vacuoles. Inhibition by calcium. *Plant J.* 11:1059–1070.

Vergani, P., D. Hamilton, S. Jarvis, and M. Blatt. 1998. Mutations in the pore regions of the yeast K^+ channel YKC1 affect gating by extracellular K^+. *EMBO J.* 17:7190–7198.

Walker, D. J., R. A. Leigh, and A. J. Miller. 1996. Potassium homeostasis in vacuolate plant cells. *Proc. Natl. Acad. Sci. USA.* 93:10510–10514.

Ward, J. M., and J. M. Schroeder. 1994. Calcium-activated K^+ channels and calcium-induced calcium release by slow vacuolar ion channels in guard cell vacuoles implicated in the control of stomatal closure. *Plant Cell.* 6:669–683.

Watson, M. B., and R. L. Malmberg. 1996. Regulation of *Arabidopsis thaliana* (L.) Heynh Arginine decarboxylase by potassium deficiency stress. *Plant Physiol.* 111:1077–1083.

Zhang, Q., F. A. Smith, H. Sekimoto, and R. J. Reid. 2001. Effect of membrane surface charge on nickel uptake by purified mung bean root protoplasts. *Planta.* 213:788–793.

Zhou, Y., J. H. Morais-Cabral, A. Kaufman, and R. MacKinnon. 2001. Chemistry of ion coordination and hydration revealed by a K^+ channel-Fab complex at 2.0 Å resolution. *Nature.* 414:43–48.